Original Study **Open Access**

Piotr Kowalczyk*

Resonance of a structure with soil elastic waves released in non-linear hysteretic soil upon unloading

https://doi.org/10.2478/sgem-2022-0015
received October 20, 2021; accepted April 22, 2022.

Abstract: High-frequency motion is often observed in small-scale experimental works carried out in flexible containers under simplified seismic loading conditions when single harmonic sine input motions are introduced at the base of a soil specimen. The source of the high-frequency motion has often been sought in experimental inaccuracies. On the other hand, the most recent numerical studies suggested that high-frequency motion in the steady-state dynamic response of soil subjected to harmonic excitation can also be generated as a result of soil elastic waves released in non-linear hysteretic soil upon unloading. This work presents an example of a finite element numerical study on seismic soil–structure interaction representative of an experimental setup from the past. The results show how high-frequency motion generated in soil in the steady-state response, apparently representative of soil elastic waves, affects the steady-state response of a structure, that is, it is presented how the structure in the analysed case resonates with the soil elastic waves. The numerical findings are verified against the benchmark experimental example to indicate similar patterns in the dynamic response of the structure.

Keywords: finite element modelling; earthquake engineering; wave propagation; soil dynamics; soil non-linearity.

1 Introduction

High-frequency components of a regular pattern of ω, 3ω, 5ω, etc. (where ω is the driving frequency) in spectral response are often observed in horizontal accelerations registered in experimental works on shaking tables, either in 1g loading environment (e.g. Abate & Massimino, 2016) or in centrifuges (e.g. Kutter et al., 2019), even when a soil specimen is subjected to single-frequency sinusoidal input motion introduced at the specimen base. Typically, high-frequency motion is associated with the imperfections of experimental setups (e.g. Brennan et al., 2005; Madabushi, 2014). On the other hand, some previous numerical studies (e.g. Pavlenko, 2001; Mercado et al., 2018) suggested that high harmonics evaluated in the spectral response of soil and showing a regular pattern of ω, 3ω, 5ω, etc. can be related to soil non-linearity modelled with hysteretic stress–strain behaviour, which causes a distortion of a propagating sinusoidal wave towards a *square wave*. Such wave distortion was shown by Mercado et al. (2018) to lead to a pattern of *exponential decay* of high harmonics in spectral response, that is, consecutive harmonics 3ω, 5ω, etc. are present with decreasing amounts (as representative of the description of a *square wave* in spectral response). A more specific conclusion on the presence of high harmonics in spectral response was drawn by Veeraraghavan et al. (2019), who recognised different shapes of the stress–strain curve (i.e. different non-linearity types) in the modelling of soil constitutive behaviour as sources of such high harmonics. Moreover, the most recent advanced numerical studies (Kowalczyk, 2020; Kowalczyk & Gajo, 2022) show a novel idea in the stress wave propagation and an introductory proof that high-frequency content observed in soil can be a result of the propagation of unloading waves. In detail, the latter work (Kowalczyk & Gajo, 2022) shows in numerical studies and by comparison with some shear stack experiments from the past (Dar, 1993; Durante, 2015) how unloading elastic waves can potentially be released upon unloading/reloading in the steady-state response in a non-linear material of hysteretic stress–strain behaviour, that is, such as soil. The suggested idea of the existence of elastic waves in the steady-state response is novel since the presence of elastic waves is recognised solely in the case of transient dynamic response (e.g. Kramer, 1996). To sum up, there are some research studies showing the source of high-frequency content in non-linear soil; nevertheless,

***Corresponding author: Piotr Kowalczyk,** Independent Researcher, formerly Department of Civil, Environmental and Mechanical Engineering, University of Trento, Trento, Italy, E-mail: pk.piotrkowalczyk.pk@gmail.com, ORCID: 0000-0003-0777-6429

the studies on the impact of soil-generated high-frequency motion on the structural response received very little attention and were only very briefly shown, mainly in relation to the response of kinematic piles, in other works of the author (Kowalczyk, 2020, 2021; Kowalczyk & Gajo, 2022).

This paper presents initial evidence of how a simple structure can exhibit resonance with high-frequency soil elastic waves generated in the steady-state response of soil subjected to harmonic excitation. To this aim, a 3D finite element numerical study representative of a typical experimental setup for a soil specimen placed in a shear stack container and subjected to seismic loading is analysed. The numerical model investigates the steady-state response of an elastic single degree of freedom (SDOF) structure when the soil specimen is subjected to single harmonic sinusoidal input motion at soil base. An advanced soil constitutive model, namely, the hypoplastic sand model (Von Wolffersdorff, 1996) with intergranular strain (Niemunis & Herle, 1997), is used to ensure a reliable representation of the complex non-linear soil behaviour. Results show that high-frequency motion, apparently representative of soil elastic waves, is generated within the soil in the steady-state response and the SDOF structure resonates with this high-frequency motion. The numerical findings are supported by comparisons with a relevant experimental example from the past (Durante, 2015).

2 Methodology

2.1 Experimental setup (Durante, 2015)

This work presents results of a finite element numerical simulation of a case of soil–structure interaction and compares this numerical study against an example of a benchmark experimental shear stack test from the past (Durante, 2015). The numerical model includes a group of five piles embedded in dry sand to represent the geometry of the experimental setup (Figure 1).

The soil in the experimental setup was placed in a flexible soil container called shear stack. The shear stack container is built of alternating layers of eight aluminium rings and rubber bands in between, thus approximating flexible lateral boundary condition for soil subjected to shearing. The relative density of dry Leighton Buzzard sand in the experimental work was relatively uniform throughout the soil height and varied only slightly from around 25% in the top part to 40% at the bottom part (Durante, 2015). The natural frequency of the dry sand placed inside the shear stack was measured to be around 25–30 Hz (depending on the amplitude of the input motion), which is much greater than the natural frequency of the empty shear stack of approximately 6 Hz, as shown in case of both values by Durante (2015). Thus, this difference in the natural frequencies guarantees that the soil rules the mechanical behaviour in the dynamic soil–shear stack system, as explained by Bhattacharya et al. (2012). The piles were modelled with 750-mm-long aluminium tubes of an external diameter of 22 mm (thickness 0.7 mm), and the pile head conditions included a case of three closer piles being joined together by means of a rigid pile cap. In the middle of the pile cap, a single degree of freedom (SDOF) structure was placed by means of a 100-mm-high aluminium column (rectangular section 3 × 12 mm) and a total mass on the top of the column of approximately 200 g (accounting for the actual added mass, the mass of an accelerometer and fixing devices). The soil-compliant natural frequency of such an oscillator was shown to be around 25 Hz (Durante, 2015), thus being close to the soil natural frequency. The input motion was applied as 5 Hz sine motion of the intended maximum horizontal acceleration of 0.063 g. Finally, note that the experimental measurements were filtered out using a low-pass 80-Hz filter (Butterworth, fifth order). Thus, the same procedure is applied to the computed accelerations in the numerical simulations for consistency.

2.2 Finite element model

The 3D finite element model has been run using Abaqus software (Dassault Systèmes, 2019). Using the fact of the symmetry of the experimental setup (as shown in Figure 1b), only a half of the experimental setup has been modelled in order to reduce the computational time. The model geometry and the chosen mesh are shown in Figure 2. No upscaling procedure has been applied to the numerically modelled experimental setup, and the dimensions of the finite element model are the same as those of the experimental model (Figure 1). Note that the rigid pile cap between the three closer piles (Figure 1) has not been modelled explicitly in the numerical model (Figure 2). Instead, the presence of the pile cap has been simulated by constraining the heads of the three piles to enforce equivalent lateral movements and no rotations of the pile heads, thus mimicking the presence of the rigid pile cap. In addition, masses have been added on each of the pile heads to account for the pile cap weight.

The numerical study assumes a single soil layer being modelled rather than a bilayered soil profile of slightly

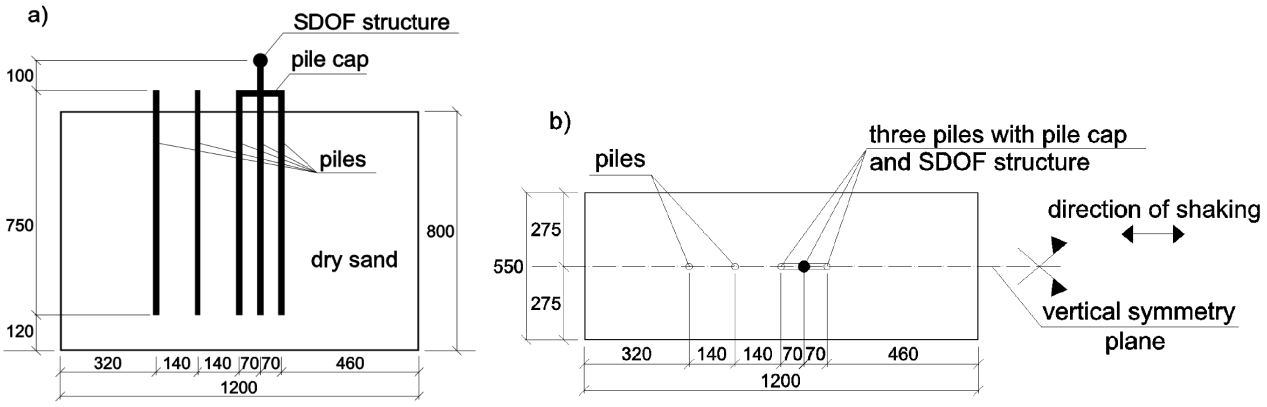

Figure 1: Geometry of numerically modelled experimental setup with a single degree of freedom (SDOF) structure: a) long side view, b) plan (dimensions in mm).

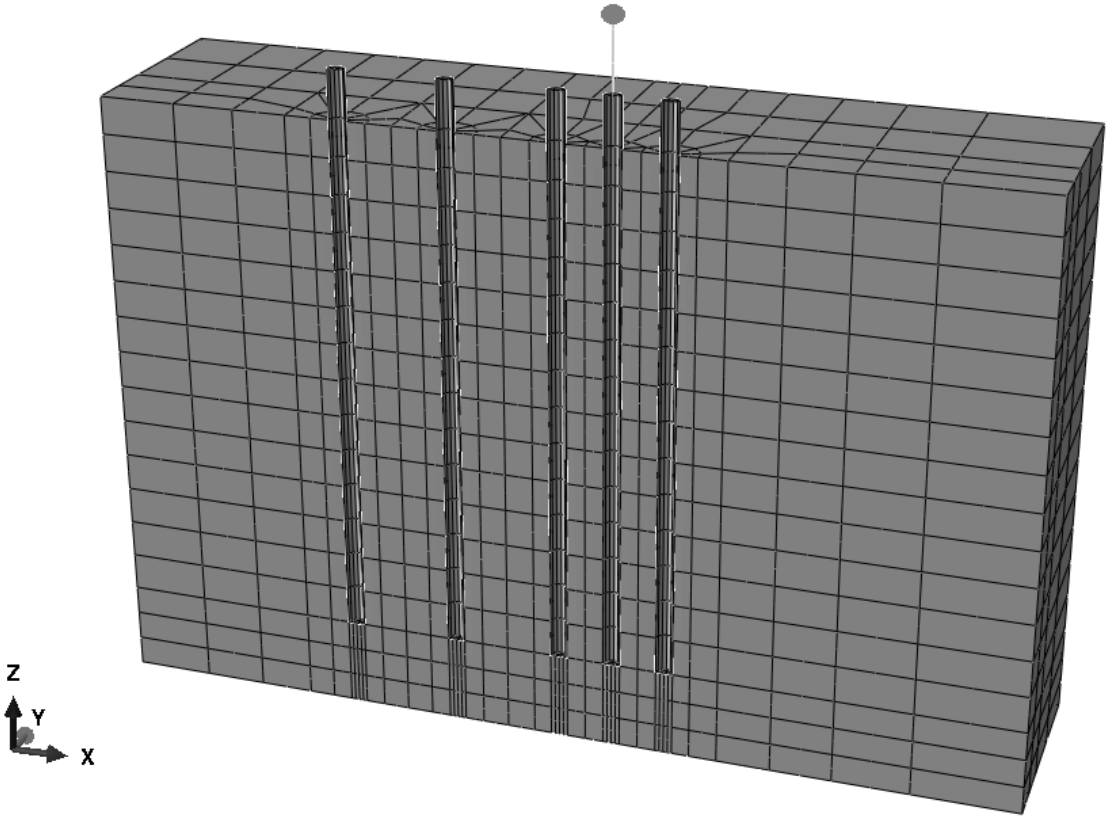

Figure 2: Mesh discretisation used in the 3D finite element model.

varying relative densities used in the experimental setup (Durante, 2015). Therefore, a homogenous soil layer has been modelled numerically to be representative of Leighton Buzzard sand, fraction E of the following soil geotechnical properties: γ_s = 2647 kg/m^3, e_{min} = 0.613, e_{max} = 1.014, D_{10} = 0.095, D_{50} = 0.14 (Tan, 1990). The initial K_0 condition has been assumed to be equal to 0.5 as deemed appropriate for dry sand at low mean effective stresses (Stroud, 1971). Note that based on appropriate parametric studies (Kowalczyk, 2020), the assumption of modelling a single homogenous soil layer was shown to be negligible when discussing the origin of high-frequency motion due to soil elastic waves released upon unloading, and this aspect is not further presented in this paper for brevity.

The finite element model has been run in three stages: first stage- geostatic stage, that is, static analysis to obtain static equilibrium in soil; second stage- static loading stage to account for the masses of the pile caps, the column supporting the structure and the structure; third stage- dynamic loading stage with acceleration time history.

2.2.1 Discretisation

The size of a quadratic element in the discretisation of soil has been chosen in a way to fulfil the minimum of the standard 'rules of thumb' to ensure accurate stress wave propagation in soil. The element size has been calculated from the propagation of an elastic wave for the slowest wave (i.e. for G_0 of approximately 3 MPa in the superficial soil) and the highest frequency (80 Hz to account for most important high frequencies) which resulted in the maximum distance between two nodes to be 0.06 m. This has been subsequently reduced to 0.025 m (quadratic element size of 0.05 m) in order to account for plasticity developing in soil, that is, lower stiffness and, therefore, slower velocities of propagating waves, leading to more strict meshing rules (Watanabe et al., 2017). Moreover, parametric studies on the mesh size, not shown in this work for brevity, were carried out (Kowalczyk, 2020) and confirmed the accuracy of the chosen mesh size for soil discretisation.

2.2.2 Boundary conditions

The boundary conditions in the finite element model have been defined at the base and the side nodes of the soil. The base nodes have been constrained in Z direction. The shear stack has not been physically introduced in discretisation, as its behaviour was shown previously to be negligible (Dietz & Muir Wood, 2007). Instead, tie connectors have been used on the short sides of the soil specimen to provide periodic boundary conditions and the nodes on the long sides have been constrained in Y direction.

Finally, sinusoidal input motion of 5 Hz frequency and the maximum amplitude of horizontal acceleration of 0.063 *g* has been introduced at the soil base in a smooth manner and with steadily increasing amplitude to reduce the presence of soil elastic waves generated due to transient dynamic response. In any case, the results from the 3D numerical model are presented when the steady-state dynamic response is reached, therefore they are not affected by the transient dynamic response.

2.2.3 Constitutive models

The soil constitutive model used in this study to model soil non-linear behaviour is a hypoplastic sand model presented by Von Wolffersdorff (1996) with the intergranular strain concept introduced in order to account for small strain stiffness (Niemunis & Herle, 1997), and subsequently updated by Wegener (2013), and Wegener & Herle (2014) to improve further predictions of accumulation of cyclic strains. Generally, hypoplasticity is a mathematical formulation that develops from hypoelasticity (Kolymbas, 1985). A particular feature of hypoplasticity is a rate-type constitutive law presented as a non-linear tensorial function. The use of a single tensorial equation results in a relatively simple formulation with no need to introduce the ingredients of classical elastoplasticity models, such as yield surfaces or consistency condition. Nevertheless, the hypoplastic sand model accounts for the most important characteristics of soil, such as barotropy, pycnotropy and the critical state (Mašín, 2018). Moreover, high-fidelity numerical studies on cyclic soil behaviour under seismic loading conditions can be expected, as shown in the past. For example, Hleibieh et al. (2014) showed that the hypoplastic sand model reproduced accurately the free field response and qualitatively the measured settlements and the response of a tunnel embedded in dry soil, whereas Hleibieh & Herle (2019) validated the hypoplastic sand model on experimental work on saturated soil, showing successful simulations of seismic soil behaviour.

The model formulation coded in a Fortran subroutine and used in this work was as provided in the User MATerial (UMAT) format at the *soilmodels.info* webpage (Gudehus et al., 2008), with only a slight modification in the model formulation due to the introduction of an additional model parameter (Wegener, 2013; Wegener & Herle, 2014) as explained above. Details on the formulation of the hypoplastic sand model are omitted in this work. The interested reader is addressed to the cited references regarding the actual formulation of the constitutive model.

The structural elements have been modelled with a linear elastic material with the properties of aluminium to be fully representative of the experimental assumptions.

The interface between the soil and the piles has been modelled as frictional and allowing a gap opening between the soil and piles. A typical value of 0.5 has been defined for the coefficient of friction between the piles and soil, as typically assumed for steel piles embedded in granular soil (e.g. Uesugi & Kishida, 1986).

2.2.4 Calibration of the hypoplastic sand model

The calibration of the hypoplastic sand constitutive model for the shear stack simulation followed the guidance specified by Dietz & Muir Wood (2007) for soil modelling in shear stack studies. The calibrated model parameters are shown in Table 1. The initial void ratio has been set to 0.91 and the sand weight to 1332 kg/m^3 to be approximately representative of the experimental setup. Figure 3 shows the G/G_0 stiffness degradation curves predicted by the calibrated hypoplastic sand model and recommended by Dietz & Muir Wood (2007). Generally, the chosen calibration of the hypoplastic sand model results in the stiffness degradation curve fitting within the recommended limits (Seed & Idris, 1970) with only a slight misfit outside the recommended range for strain levels greater than 10^{-3}. Nevertheless, such strain levels are induced only for large-amplitude input motions and not for the one used in this study.

More details regarding the chosen calibration method, model parameters and the validation of a similar calibration of the hypoplastic sand constitutive model can be found in the previous work of the author (Kowalczyk, 2020). Moreover, Appendix A shows an example of a cyclic simple shear test simulated by the hypoplastic sand model with the model calibration as per Table 1 and compared with experimental data from literature (Shahnazari & Towhata, 2002).

2.2.5 Typical response of the hypoplastic sand model to s-wave propagation

A brief presentation of typical numerical results for free field response to s-wave propagation is presented in Figure 4. The results are obtained with the chosen calibration of the hypoplastic sand model in a simple numerical study of a 0.8-m-high soil column (32 quadratic finite elements of the size of 0.025 m). Indeed, this numerical example shows the essence of the potential presence of soil elastic waves released upon unloading in the steady-state part of dynamic response (as per the patterns shown in more detail in a parallel work by Kowalczyk & Gajo, 2022). The soil elastic waves are particularly visible for loading cases when the driving frequency (5 Hz) of the input motion is smaller than the soil natural frequency (approximately 25 Hz), such as the case presented in Figure 4.

It can be observed in Figure 4 how smoothly introduced input motion at the base of the soil column results in a clear presence of high-frequency motion at the top of the soil column (in the computed horizontal accelerations

Table 1: Calibration of the model parameters for the hypoplastic sand model.

	Parameter	Description	Value
Basic hypoplastictiy	φ_c	Critical friction angle	33.0
	h_s	Granular hardness (kPa)	2.5×10^6
	n	Stiffness exponent ruling pressure-sensitivity	0.42
	e_{d0}	Limiting minimum void ratio at p = 0 kPa	0.613
	e_{c0}	Limiting void ratio at p = 0 kPa	1.01
	e_{i0}	Limiting maximum void ratio at p = 0 kPa	1.21
	α	Exponent linking peak stress with critical stress	0.13
	β	Stiffness exponent scaling barotropy factor	0.8
Intergranular strain concept	R	Elastic range	0.00004
	m_R	Stiffness multiplier	4.0
	m_T	Stiffness multiplier after 90° change in strain path	2.0
	β_R	Control of rate of evolution of intergranular strain	0.8
	χ	Control on interpolation between elastic and hypoplastic response	0.5
	ϑ	Control on strain accumulation	5.0

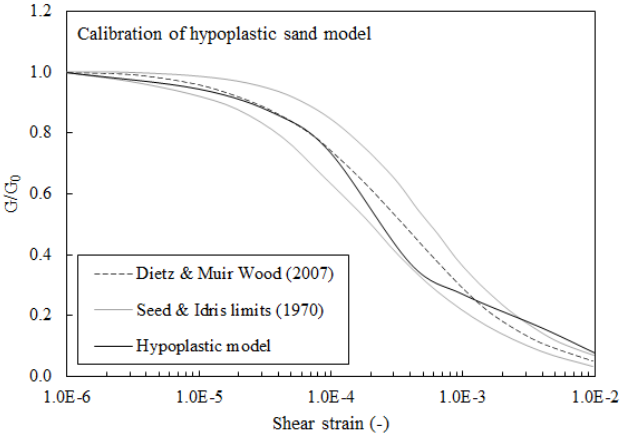

Figure 3: Calibration of the hypoplastic sand constitutive model in terms of shear stiffness degradation G/G_0 against shear strain.

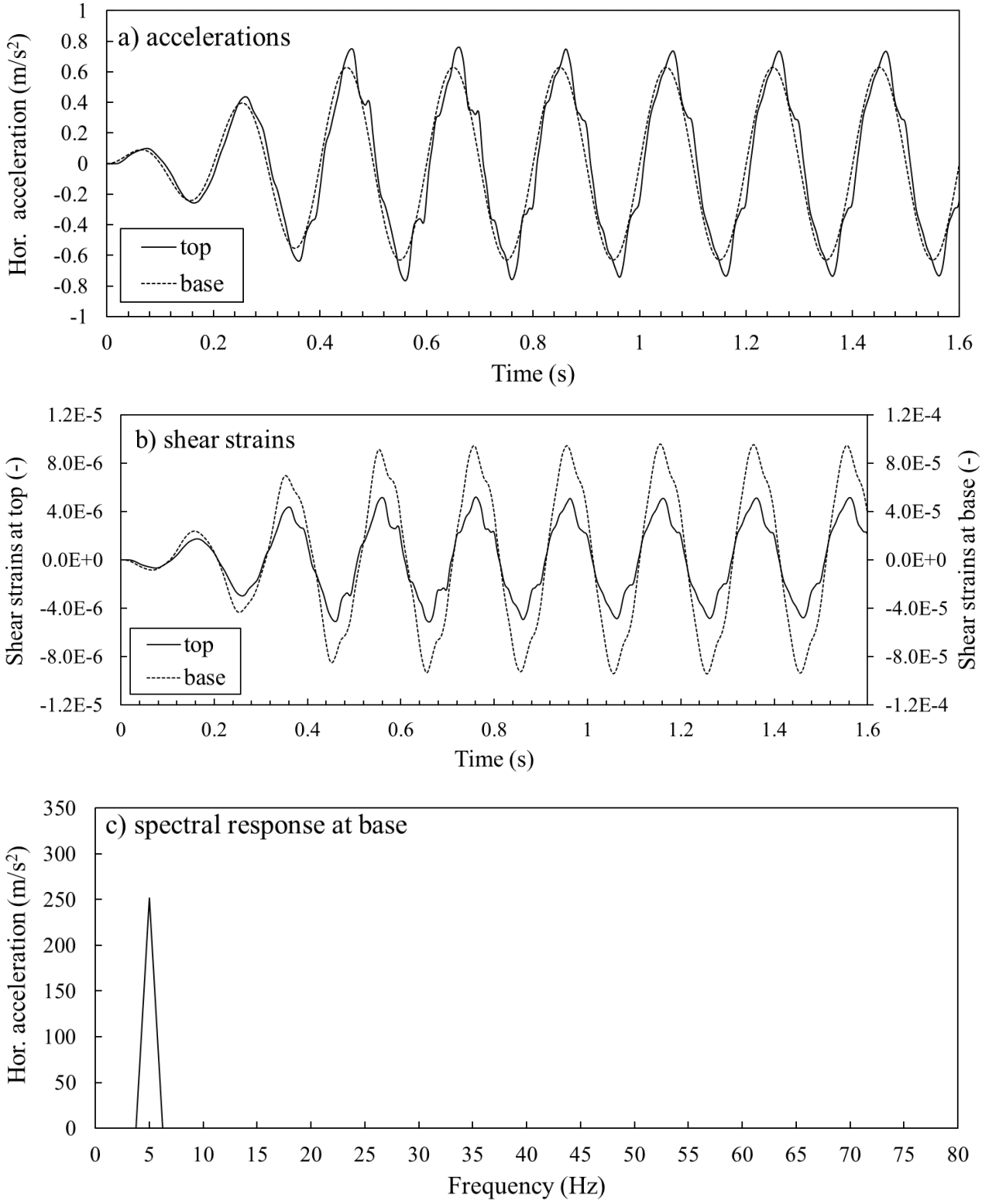

Figure 4: Free field response computed for the soil column with the chosen calibration of the hypoplastic sand model (Table 1): a) horizontal accelerations, b) shear strains, c) spectral response for horizontal accelerations at the soil base, d) spectral response for horizontal accelerations at the soil top, e) stress–strain behaviour.

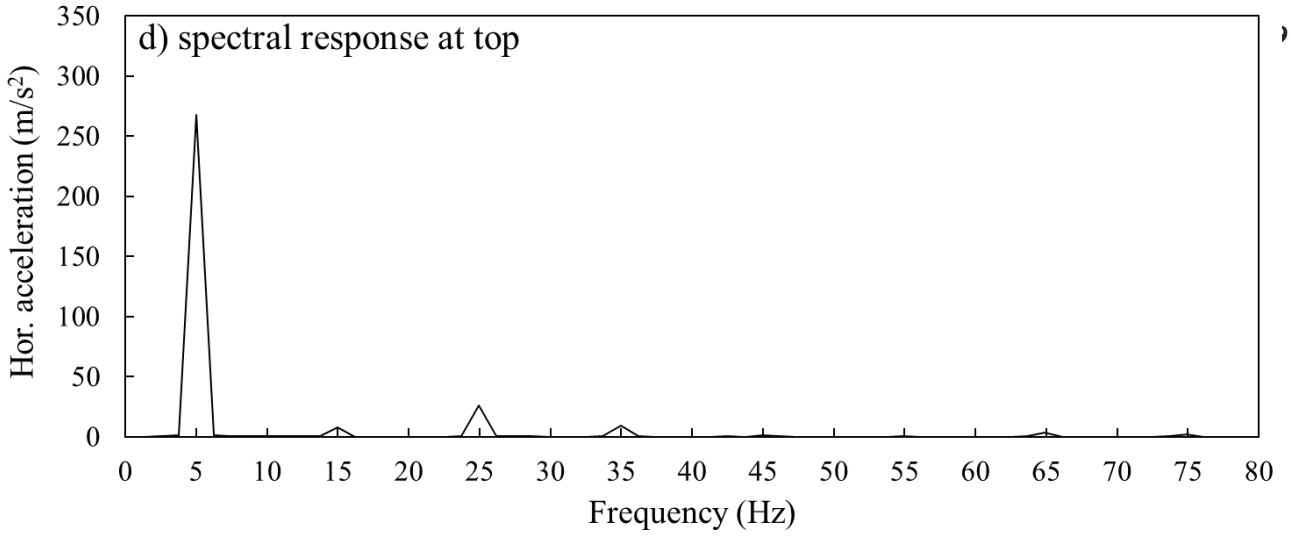

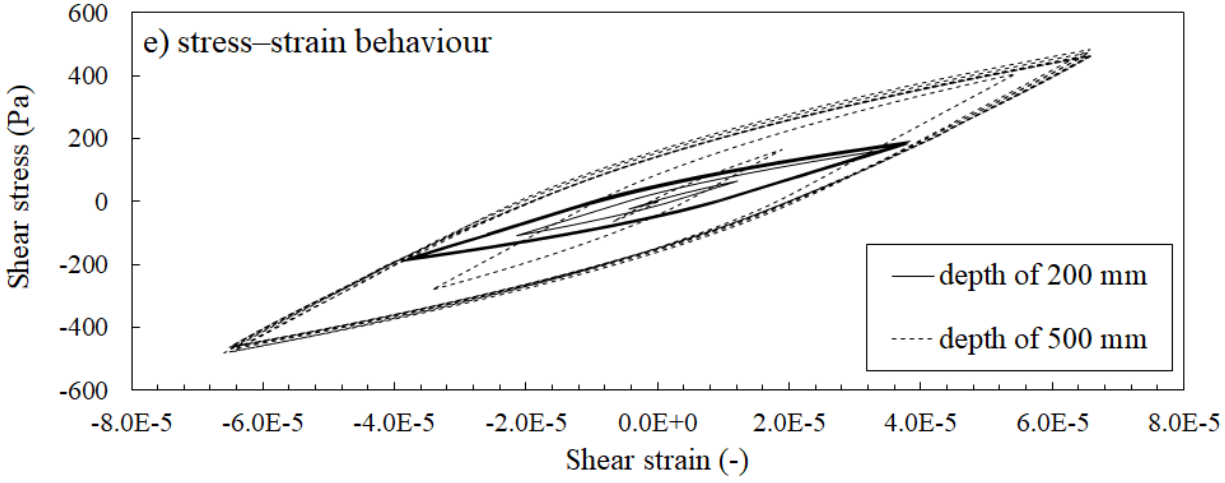

Continued **Figure 4:** Free field response computed for the soil column with the chosen calibration of the hypoplastic sand model (Table 1): a) horizontal accelerations, b) shear strains, c) spectral response for horizontal accelerations at the soil base, d) spectral response for horizontal accelerations at the soil top, e) stress–strain behaviour.

in Figure 4a and in the computed shear strains in Figure 4b) in, what apparently appears to represent, the steady-state response (i.e. after approximately 1.0 s of motion). It is reminded that for a general case, transient response diminishes with time depending on the energy dissipation present in a system, and, in theory, the transient response never disappears completely, but, in practice, it becomes so fractional that it can be neglected when the consecutive cycles of response appear to repeat each other. This approach has been adopted in this study to identify the steady-state response. Thus, the computed response after approximately 1.0 s of motion can be reasonably considered as representative of the steady-state response, since the consecutive sine cycles appear to replicate each other (Figure 4a and b).

Figure 4c and 4d shows the acceleration spectral response evaluated at the soil base and soil top, respectively, for the steady-state dynamic response of soil, that is, after 1.0 s, when the effects induced due to transient dynamic response are fractional and negligible as assumed above. The pattern of higher harmonics evaluated at soil top and shown in Figure 4d is clearly different from the *exponential decay* pattern (Mercado et al., 2018) explained before. Instead, the evaluated spectral response in the steady-state response predicts strong presence of higher harmonic of 25 Hz that is representative of soil elastic waves.

Finally, Figure 4e presents the computed mechanical behaviour of soil in terms of shear stress against shear strain at two depths of approximately 200 and 500 mm. It can be observed that the calibrated hypoplastic sand model correctly predicts expected hysteretic behaviour in the soil column.

3 Results

The results of the computed horizontal accelerations and displacements obtained from the 3D numerical model and compared with the benchmark experimental data (Durante, 2015) are shown in Figures 5–7. Firstly, Figure 5 presents the horizontal accelerations in free field for the steady-state dynamic response of soil. It can be observed in Figure 5a that for the input motion of a single harmonic sine at base, the perfect shape of the sine wave is regularly distorted in the numerical computations and experimental data at soil surface within the steady-state cycles (i.e. practically, the same response is computed and recorded in each of the sine cycles without any visible trace of damping out high frequencies, as would be expected in case of elastic waves due to transient response). This regular distortion indicates the presence of higher frequencies of motion larger than the driving frequency of 5 Hz. Figure 5b presents the evaluated spectral response and reveals noticeable presence of the higher harmonic of 25 Hz (i.e. soil natural frequency), and thus is similar to the response shown in Figure 4. Note that the free field response presented in Figure 5 confirms the accuracy of the chosen mesh size in the 3D numerical model, as the numerical results from the 3D model match the results shown in Figure 4 (for a soil column discretised with 32 quadratic elements).

Figure 6 shows a comparison between the computed and measured relative horizontal displacements in free field at the soil surface. Some inconsistency in the amplitude of motion can be observed; however, the values remain within the same order of magnitude and the sine wave is regularly distorted in subsequent loading cycles of the steady-state response in the simulation and the experiment, thus confirming the findings presented for the computed and measured horizontal accelerations in free field.

Figure 7 shows the horizontal accelerations computed and measured at the top of the SDOF structure. It can be observed that the structure vibrates with the frequency of the input motion (5 Hz). However, in addition, strong presence of high-frequency motion of 25 Hz can be observed. Similar to the results shown in free field, the high-frequency motion does not diminish in amplitude with subsequent sine cycles. Apparently, the 25-Hz frequency wave is introduced in each sine cycle, thus cannot be the result of soil elastic waves due to transient response. It appears that the 25-Hz frequency is more amplified in the experimental measurements than in the numerical simulations. The slight difference in the amount of the second dominant frequency of motion of the structure can be the result of various modelling assumptions which can differ between the numerical and experimental studies, for example, the amount of the induced non-linearity in the soil response or inaccuracy in approximately evaluated mass placed on the top of the SDOF structure. Nevertheless, the second dominant frequency of motion computed and recorded on the structure is always 25 Hz, which is the natural frequency of the soil and the modelled structure. Therefore, it appears that soil elastic waves present in the steady-state response of free field can cause resonance of the analysed structure with these waves.

To sum up the results shown in Figures 5–7, the analysed numerical case shows how high-frequency motion of 25 Hz, not present in the input motion at base and apparently representative of soil elastic waves, is generated in the soil and present on soil surface (Figures 5 and 6) and how this high-frequency motion affects the structural response (Figure 7). It is evident from the studied example that in such a special case, when the structural and soil natural frequencies are similar (such as herein), the structure can be excited into resonance with the soil-released elastic waves in the steady-state response. Such structural response can be thought as an example of *superharmonic resonance*, as shown before for a different non-linear frictional system by Vitorino et al. (2017), where a structure resonated with a higher harmonic of motion generated by the non-linear system and not present in input motion. Moreover, it appears that an elastic structure placed in soil can act as an additional *measuring instrumentation* and provides further evidence to support the idea of the release of soil elastic waves in the steady-state response of non-linear hysteretic soil. In other words, if soil elastic waves were not released and were physically not present in the steady-state response of hysteretic soil, the structure would simply vibrate with the single driving frequency of the input motion, since no other waves were present in the system (the elastic waves due to transient response would always be damped out). Nevertheless, this does not seem to be the case either for the presented numerical study or for the experimental example; therefore, the presented results strengthen the idea of the possible release of soil elastic waves in the steady-state response for materials such as soils characterised by non-linear hysteretic stress-strain behaviour.

In regard to the experimental work (Durante, 2015) used as a point of reference in this paper, it is recalled that it was dedicated to the investigation of kinematic and inertial interaction of piles with soil and not to high-frequency motion. As a result, certain experimental

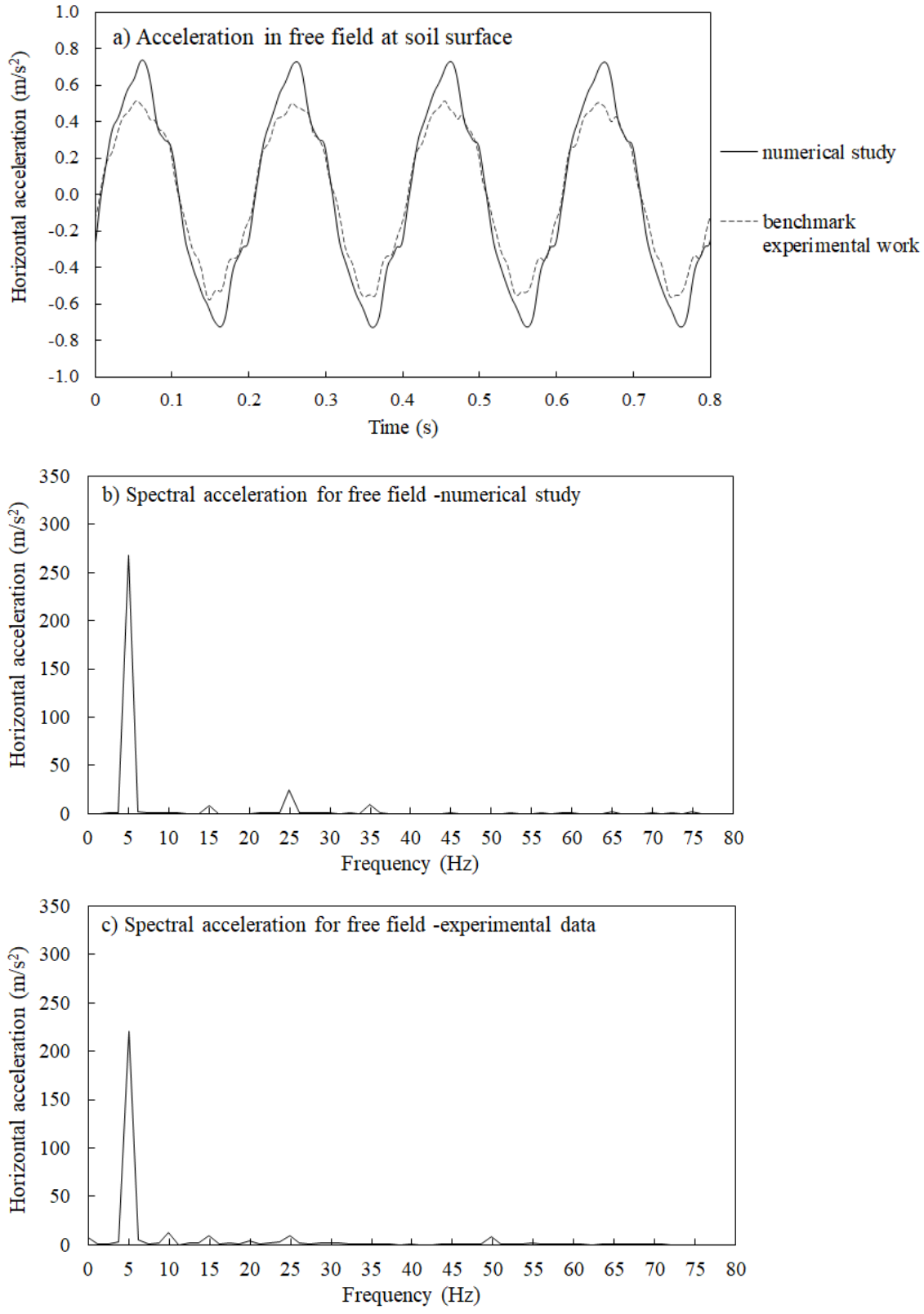

Figure 5: Comparison of the computations and the experimental measurements (Durante, 2015) in free field in the steady-state response: a) horizontal accelerations, b) evaluation of the spectral response of the computed horizontal accelerations, c) evaluation of the spectral response of the horizontal accelerations in the experiment.

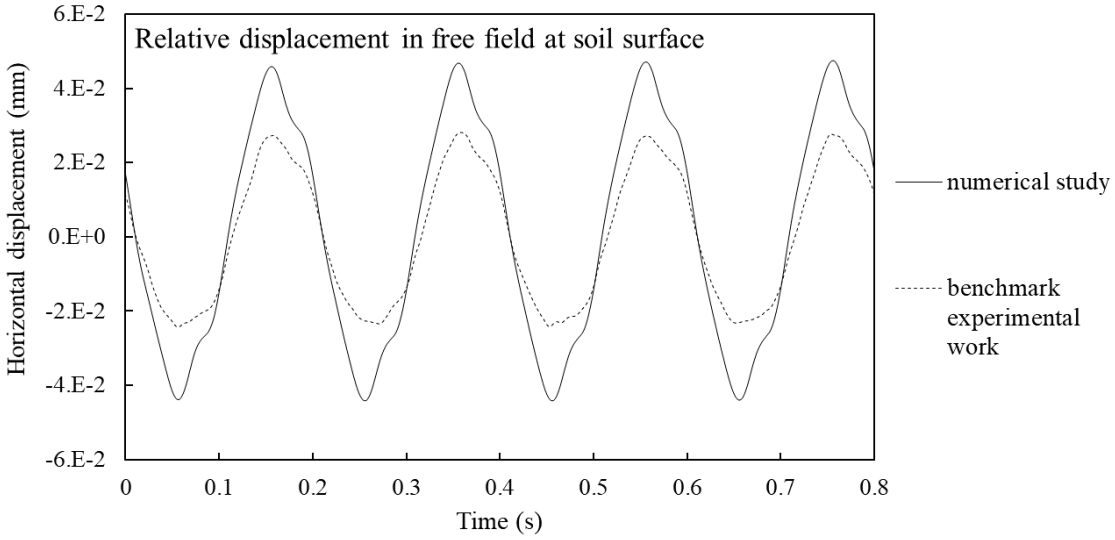

Figure 6: Comparison of relative horizontal displacements between the computations and the experimental measurements (Durante, 2015) obtained in free field in the steady-state response.

assumptions, such as slight difference in relative density from 25% (top of soil) to 40% (bottom of soil), could result in the introduction of additional waves into the soil–structure system. This problem had been addressed by the author in his other work (Kowalczyk, 2020), where relevant parametric numerical studies showed that modelling soil as a single-layered or a bilayered soil profile had negligible influence on the results regarding the soil-generated high-frequency motion. Generally, it is reminded that the experimental work encounters a number of imperfections, such as approximated lateral boundary conditions (due to the use of alternating rigid aluminium rings and flexible rubber bands), accumulation of plastic strains (due to loading history of previously run experimental tests) or imperfect input motions (due to noise from the electric current), all of which may affect the phenomena of high-frequency motion. On the other hand, the numerical study simulates a perfect experimental setup, where the experimental imperfections are eliminated. Therefore, based on the generally satisfactory comparisons between the numerical and experimental results presented herein, the above-listed experimental imperfections may likely be considered as negligible when studying the observed phenomena of high-frequency motion.

Regarding the numerical results shown in this work, it is important to highlight that these are not dependent on the chosen constitutive model. The other works of the author (Kowalczyk, 2020; Kowalczyk & Gajo, 2022) showed that the same patterns of high-frequency motion computed in soil (and representative of soil elastic waves) can be obtained with different soil constitutive models. In fact, any constitutive model of non-linear hysteretic stress-strain behaviour (i.e. a hypoplastic or elastoplastic; depth-dependent or depthindependent model) would be able to reproduce the same general patterns of numerical results as presented herein.

Finally, it can be stated that the presented findings on soil-generated high-frequency motion representative of soil elastic waves and affecting the structural dynamic response are of novel character, and therefore should deserve more attention of the earthquake geotechnical engineering community. To this aim, further studies including detailed dedicated research and possibly analysing more realistic scaled earthquake input motions would be required to confirm explicitly and to quantify the findings shown in this paper.

4 Conclusions

To sum up, this paper has presented the importance of soil-generated high-frequency motion, apparently representative of soil elastic waves released in non-linear hysteretic soil, on structural dynamic response in the steady state. The conducted numerical study and the example of the benchmark experimental data from the past have shown initial evidence that a simple structure of a natural frequency close to the soil natural frequency can exhibit resonance with soil elastic waves released in the steady-state response when the soil is excited at base with simple harmonic motion of the driving frequency different from the soil natural frequency.

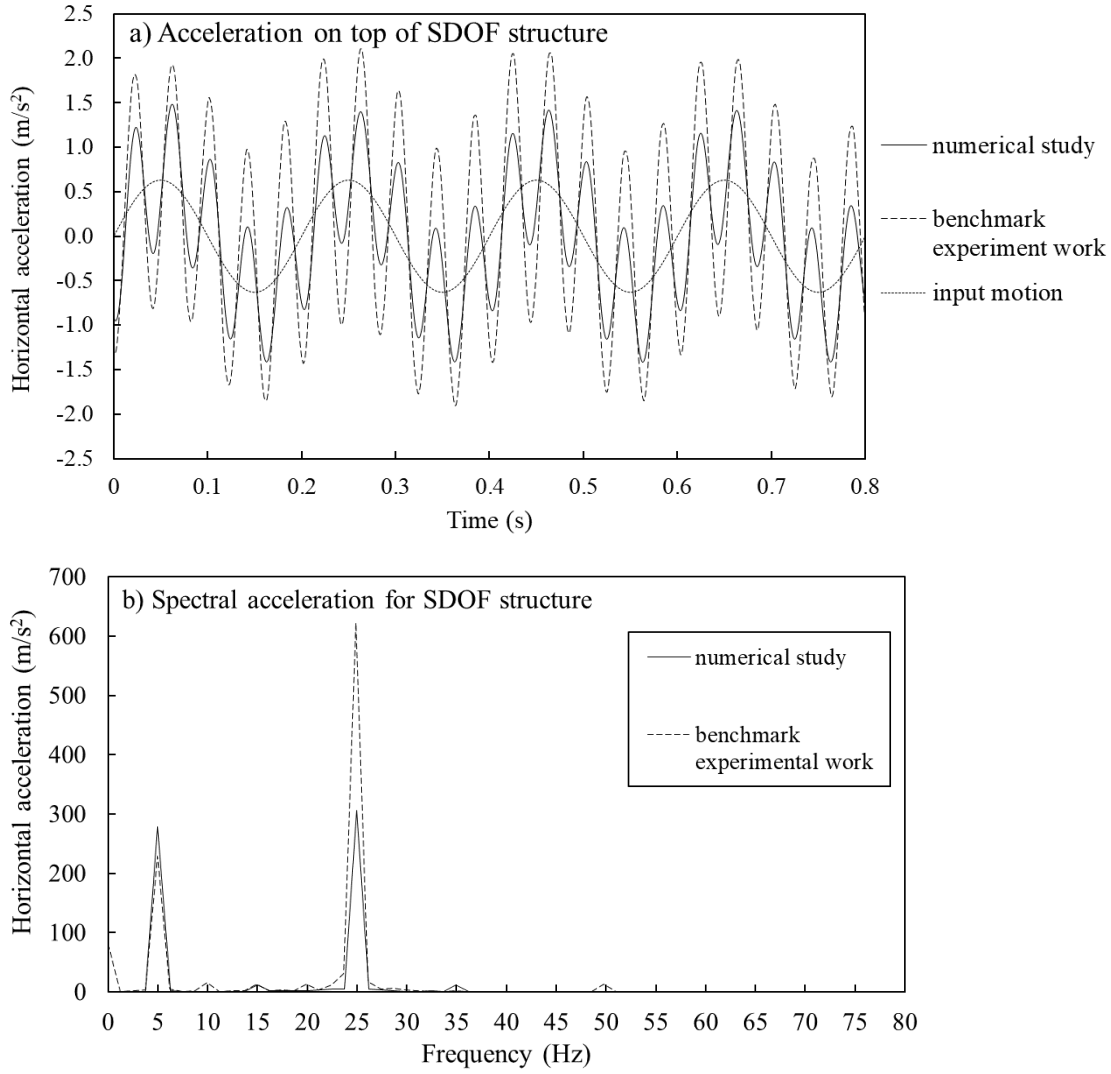

Figure 7: Comparison of the computations and the experimental measurements (Durante, 2015) obtained at the top of the structure in the steady-state response: a) horizontal accelerations, b) evaluation of the spectral response of the computed and measured horizontal accelerations.

Acknowledgements: The author would like to acknowledge University of Trento for provision of computational resources.

The author would like to thank Dr. Maria Giovanna Durante (University of Texas) and Prof. Luigi di Sarno (University of Liverpool) for provision of data of the examples of the experimental work.

References

[1] Abate, G., Massimino, M., R. (2016). Dynamic soil-structure interaction analysis by experimental and numerical analysis. Rivista Italiana di Geotecnica 2/2016.

[2] Bhattacharya, S., Lombardi, D., Dihoru, L., et al. (2012). Model container design for soil-structure interaction studies. *In: Role of Seismic Testing Facilities in Performance-Based Earthquake Engineering*. Springer, Dordrecht, 135-158.

[3] Brennan, A.J., Thusyanthan, N. I., Madabhushi, S.P.G. (2005). Evaluation of shear modulus and damping in dynamic centrifuge tests. Journal of Geotechnical and Geoenvironmental Engineering 131(12), 1488-1497.

[4] Dar, A. R. (1993). Development of a flexible shear-stack for shaking table testing of geotechnical problems. PhD Thesis. University of Bristol.

[5] Dassault Systèmes (2019). Abaqus Standard software package.

[6] Dietz, M., Muir Wood, D. (2007). Shaking table evaluation of dynamic soil properties. *In proceedings of: 4th International Conference of Earthquake Geotechnical Engineering*, June 25-28, Thessaloniki, Greece, 2007.

[7] Durante, M. G. (2015). Experimental and numerical assessment of dynamic soil-pile-structure interaction. PhD Thesis. University of Naples Federico II.
[8] Gudehus, G., Amorosi, A., Gens, A., et al. (2008). The soilmodels.info project. International Journal of Numerical and Analytical Methods in Geomechanics 32(12), 1571-1572.
[9] Hleibieh, J., Wegener, D., Herle, I. (2014). Numerical simulations of a tunnel surrounded by sand under earthquake using a hypoplastic model. Acta Geotechnica 9, 631-640.
[10] Hleibieh, J., Herle, I. (2019). The performance of a hypoplastic constitutive model in predictions of centrifuge experiments under earthquake conditions. Soil Dynamics and Earthquake Engineering, 122, 310-317.
[11] Kolymbas, D. (1985). A generalized hypoelastic constitutive law. *In Proceedings of the 11th International Conference on Soil Mechanics and Foundation Engineering*, San Francisco, USA.
[12] Kowalczyk, P. (2020). Validation and application of advanced soil constitutive models in numerical modelling of soil and soil-structure interaction under seismic loading. PhD Thesis. University of Trento, http://hdl.handle.net/11572/275675
[13] Kowalczyk, P. (2021). New insight on seismic soil-structure interaction: amplification of soil generated high frequency motion on a kinematic pile. In Proceedings of the 1st Croatian Conference on Earthquake Engineering, 22-24 March, Zagreb, Croatia.
[14] Kowalczyk, P., Gajo, A. (2022).. Introductory consideration supporting the idea of the potential presence of unloading elastic waves in seismic response of hysteretic soil. Soil Dynamics and Earthquake Engineering (currently under completion, title to be confirmed).
[15] Kramer, S. L. (1996). Geotechnical Earthquake Engineering. Prentice Hall, US.
[16] Kutter, B. L., Carey, T. J., Stone, et al. (2019). LEAP-UCD-2017 Comparison of Centrifuge Test Results. *In: B. Kutter et al. (Eds.), Model tests and numerical simulations of liquefaction and lateral spreading: LEAP-UCD-2017*. New York: Springer.
[17] Madabhushi, G. S. P. (2014). Centrifuge modelling for civil engineers. Taylor & Francis Ltd.
[18] Mašín, D. (2018). Modelling of Soil Behaviour with Hypoplasticity: Another Approach to Soil Constitutive Modelling. Springer.
[19] Mercado, V., W. El-Sekelly, Abdoun, T., Pajaro, C. (2018). A study on the effect of material nonlinearity on the generation of frequency harmonics in the response of excited soil deposits. Soil Dynamics and Earthquake Engineering 115, 787-798.
[20] Niemunis, A., Herle, I. (1997). Hypoplastic model for cohesionless soils with elastic strain range. Mechanics of Cohesive-Frictional Materials 2, 279-299.
[21] Pavlenko, O. (2001). Nonlinear seismic effects in soils: numerical simulation and study. Bulletin of Seismological Society of America 91(2), 381-96.
[22] Seed, H. B., Idriss, I. M. (1970). Soil moduli and damping factors for dynamic response analysis. EERC report 70-10. University of California, Berkeley.
[23] Shahnazari, H., Towhata, I. (2002). Torsion shear tests on cyclic stress-dilatancy relationship of sand. Soils and Foundations 42(1), 105-119.
[24] Stroud, M. A. (1971). The behaviour of sand at low stress levels in the simple shear apparatus. PhD Thesis. University of Cambridge.
[25] Tan, F.S.C. (1990). Centrifuge and theoretical modelling of conical footings on sand. PhD Thesis. University of Cambridge.
[26] Uesugi, M., Kishida, H. (1986). Influential factors of friction between steel and dry sands. Soils and Foundations 26(2), 33-46.
[27] Veeraraghavan, S., Spears, R. E., Coleman, J. L. (2019). High frequency content in soil nonlinear response: A numerical artefact or a reality? Soil Dynamics and Earthquake Engineering 116, 185-191.
[28] Vitorino, M. V., Vieira, A., Rodrigues, M. S. (2017). Effect of sliding friction in harmonic oscillators. Scientific Reports 7(1), 3726.
[29] Von Wolffersdorff, P. A. (1996). A hypoplastic relation for granular materials with a predefined limit state surface. Mechanics of Cohesive and Frictional Materials 1(3), 251-271.
[30] Wegener, D. (2013). Numerical investigation of permanent displacements due to dynamic loading. PhD thesis. TU Dresden (Germany).
[31] Wegener, D., Herle, I. (2014). Prediction of permanent soil deformations due to cyclic shearing with a hypoplastic constitutive model. Geotechnik 37(2), 113-122.

Appendix A

This appendix shows the results for a cyclic simple shear test simulated by the hypoplastic sand model and compared with the experimental data by Shahnazari & Towhata (2002). The performance of the constitutive model in cyclic simple shear is of paramount importance as this is the dominant stress path in the shear stack subjected to s-wave propagation.

The laboratory test was carried out at a constant vertical stress of 98 kPa on Toyoura sand with the initial void ratio of 0.756. This test was numerically simulated with the hypoplastic sand model calibrated for Leighton Buzzard sand in the shear stack, as presented in the 'Methodology' section and Table 1.

The results presented in Figure A1 show that the calibrated hypoplastic sand model is able to reasonably well replicate the soil stress–strain behaviour and the soil volumetric changes when simulating the cyclic simple shear test.

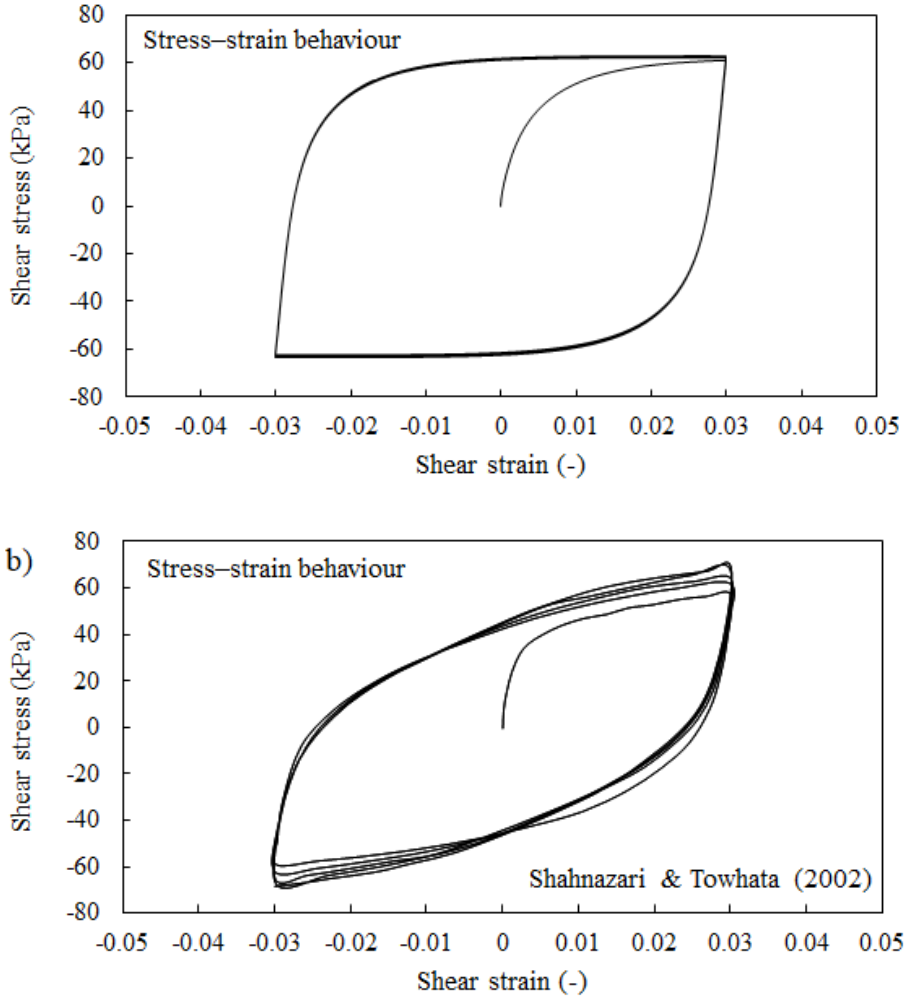

Figure A1: Comparison of a cyclic simple shear test simulated by the hypoplastic sand model and compared with experimental data from literature (Shahnazari & Towhata, 2002): a) stress–strain behaviour (simulation), b) stress–strain behaviour (experiment), c) volumetric response (simulation), d) volumetric response (experiment).

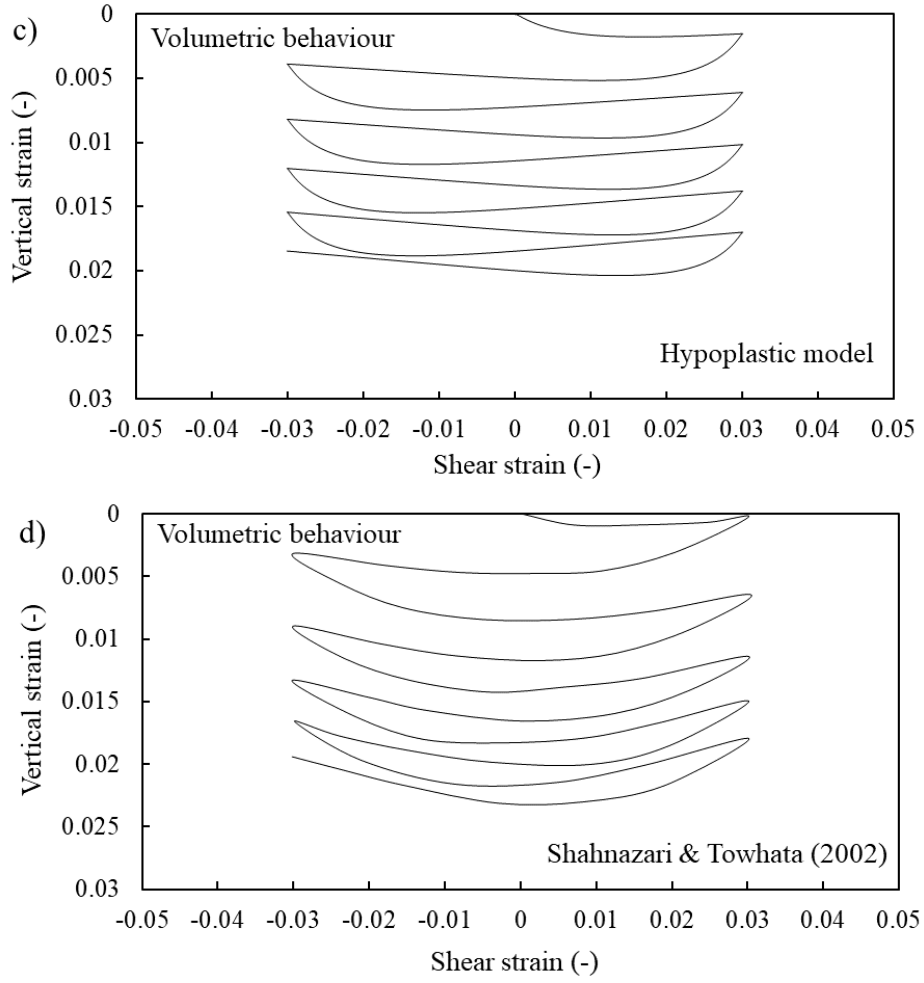

Continued **Figure A1:** Comparison of a cyclic simple shear test simulated by the hypoplastic sand model and compared with experimental data from literature (Shahnazari & Towhata, 2002): a) stress–strain behaviour (simulation), b) stress–strain behaviour (experiment), c) volumetric response (simulation), d) volumetric response (experiment).